Pollution 2021, 7(2): 377-393
DOI: 10.22059/poll.2021.313734.937

RESEARCH PAPER

Extraction of Keratin from Human Hair Waste as Adsorbent: Characterization, Thermodynamic and Kinetic Study for Removal of Chromium (VI) ions

Fereshteh Abbasi[1*], Abdolhadi Farrokhnia[2] and Zahra Abbasi[3]

1. Department of Chemistry, Ilam Branch, Islamic Azad University, Ilam, Iran
2. Department of Chemistry, College of Science, Shahid Chamran University of Ahvaz, Ahvaz, Iran
3. Faculty of Science, Ilam University, P.O.Box 69315516, Ilam. Iran

Received: 15 November 2020, Revised: 18 February 2021, Accepted: 04 March 2021

ABSTRACT
In this paper, human hair, as a waste material, was utilized in order to prepare keratin nanoparticles. The characterization of keratin nanoparticles was performed applying Transmission electron microscopy (TEM), Scanning electron microscopy (SEM), Fourier transform infrared spectroscopy (FT-IR) and X-Ray diffraction (XRD). The average diameter of keratin nanoparticles was found to be 63.7 nm, using particle size analyzer. Subsequently, the keratin nanoparticles were employed for Cr (VI) ions adsorption. The batch experiment was carried out to find the optimum conditions; i.e. contact time, pH, adsorbent dose and initial concentration of Cr (VI) ions. The adsorption capacity was extremely pH-dependent, and the maximum adsorption of Cr (VI) happened in the acidic pH range. The results demonstrated that the maximum adsorption capacity, obtained in acidic pH, was 161.29 mg/g. The equilibrium data were well fitted by Freundlich isotherm. The kinetic studies were performed with the Lagergren's first-order, Pseudo-second order, Elovich, and Intra-particle diffusion models. In this sense, in order to describe kinetic data, we came to this understanding that Pseudo-second order model was the best choice. The thermodynamic parameters of the adsorption process indicated that the Cr (VI) adsorption on keratin nanoparticles is endothermic and spontaneous.

Keywords: Cr (VI) ions, Keratin nanoparticles, Isotherm, Adsorption kinetics, Hair Waste, optimum.

INTRODUCTION

Chromium can be found in trivalent Cr(III) and hexavalent Cr(VI) ion forms in the aqueous solution (Zhang et al., 2017). While Cr(III) is a basic nutrient for human beings (especially in lipid, glucose and protein metabolism) as well as animals and plants at trace concentration (Saboori, 2017), Cr(VI) is the most toxic form whose toxicity is 300 times higher than that of Cr(III). Besides, it is mutagenic and carcinogenic to humans and other living organisms which can be due to its mobility and high solubility in the aquatic system (Liu, Leng, & Lin, 2016). Exposure to hexavalent chromium may cause mutations, DNA damage, epigastric pain, skin ulcer, liver damage, pulmonary congestion, bronchitis, and cancer (Cui, Song, Wang, & Song, 2015). It is in leather tanning, electroplating, pigment, wood preservation, manufacturing of various alloys, textile, film and photography, pulp processing and glass industry that

* Corresponding Author, Email: Abbasi519@ilam-iau.ac.ir

Chromium can be applied (Xie, Gu, Tong, Zhao, & Tan, 2015). In this regard, it is during the chrome tanning process that 40% of the unused chromium salts can be discharged in the final effluents. The admissible limit for Cr(VI) disposal to the surface waters and in drinkable water is 0.1 mg/L and 0.05 mg/L respectively, while, Cr(VI) concentration in industrial wastewater is between 0.5 to 270 mg/L(Bansal, Singh, & Garg, 2009). Consequently, it is basically significant to remove Cr (VI) from industrial wastewater. Nowadays, in order to remove Cr(VI) ions from surface water and wastewater, effective technologies, i.e. filtration, chelation, reduction, osmosis, ion exchange, electrochemical operation, solvent extraction, catalytic and photocatalytic reduction, and adsorption, can be used (Rezvani, Asgharinezhad, Ebrahimzadeh, & Shekari, 2014). However, such methods have major drawbacks such as using large amounts of reagents, incomplete metal removal, and generation of secondary waste or toxic sludge. Among these methods, adsorption process, as a low-cost and highly efficient method, is greatly applied in wastewater, containing heavy metals, treatment (Marjan et al., 2020). During recent years, in order to eliminate Cr(VI) from aqueous solutions, low-cost adsorbents such as granular and powdered Peganum Harmala (Khosravi, Fazlzadehdavil, Barikbin, & Taghizadeh, 2014), Sakura waste (Qi, Zhao, Zheng, Ji, & Zhang, 2016), treated waste newspaper (Dehghani, Sanaei, Ali, & Bhatnagar, 2016), soy hull biomass (Blanes et al., 2016), and agricultural waste (Nik Abdul Ghani et al, 2021) can be used. Currently, natural materials are available in large quantities, and the wastes in the environment can be considered as low-cost adsorbents for heavy metals (Mohsen et al., 2019). It is worth mentioning that keratin can be regarded as the main component in hair, wool, feathers, horns, and nail. Throughout their life cycle, keratin materials have also been regarded as environmentally friendly ones. Each year, the large amount (more than 5 million tons) of produced keratin waste can be traced back to butchery, the textile industry, etc. In this sense, such wastes would frequently accumulate in large volumes and, as a result, choke the drainage system. It results in a foul odor, toxic gasses, and a breeding ground for pathogens. In order to solve the problem and make them valuable, a specific system must be developed in which the keratin waste as an adsorbent be utilized (Gupta, 2014). In recent years, keratinous materials have been applied as a novel adsorbent system for the toxic pollutant (Ghosh & Collie, 2014), heavy metals(Kar & Misra, 2004), copper (II) (A. Aluigi, Tonetti, Vineis, Tonin, & Mazzuchetti, 2011) and Pb (II) from water (Sekimoto et al., 2013). This high potential of application can be due to the presence of amino acid chains on the backbone and also on the side-chain of keratin structure (Hearle, 2000; Volkov & Cavaco-Paulo, 2016)

This paper describes the extraction of keratin nanoparticles from human hair. Afterwards, the potential application of keratin nanoparticles and environmental friendly and inexpensive adsorbent for the removal of Cr (VI) ions will be investigated.

MATERIALS AND METHODS

Urea, thiourea, ethanol, acetone, tris-hydrochloride, HNO_3, HCl, NaOH, $K_2Cr_2O_7$ and 1,5-diphenyl carbazide were supplied by Merk (Germany). 2-Mercaptoethanol(2-ME) was bought from Samchon (South Korea). Cellulose dialysis tube (D9652,12kDa) was purchased from Sigma (USA).

A freeze dryer (Operon) was applied in order to perform the drying process of keratin nanoparticles. Besides, common Incubator (FSA554D) was also used to do the incubation process. Cintra 101 GBC and VERTEX70-BRUCKER were applied in order to acquire UV-visible and Fourier transform infrared spectroscopy (FT-IR) spectra, respectively. Particle size analyzer (Scatteroscopequdix) was used for nanoparticles size analysis. Scanning electron

microscopy (SEM) and Transmission electron microscopy (TEM) were performed using LEO1455VP/ SEM and EM900/TEM, respectively. Moreover, X-ray diffractometer (BW1840) was used to obtain X-ray diffraction (XRD) pattern.

As stated by Fuji and Kato, the keratin aqueous solution was extracted in accordance to the modified Shindai method (Sekimoto et al., 2013). Briefly, in order to remove the external lipid, we used ethanol to wash human hair. Chopped hair (0.8 g) was incubated with 200 mL solution, containing 5M urea, 2.6 M thiourea, 25 mM tris-hydrochloride, and 150 mM 2-mercaptoethanol at 50^{o}C for 3 days. Afterwards, it was at11000×g that we aimed at filtering the mixture and, then, centrifuging it for 20 min at room temperature. Accordingly, the dialysis was done to the obtained supernatant at 12^{o}C for 3 days using the distilled water which was changed four times a day. After dialysis, in order to recover the keratin nanoparticles powder, we aimed at lyophilizing the obtained keratin aqueous solution.

When 2.828 g of $K_2Cr_2O_7$ was dissolved in 1000 mL of deionized water, it resulted in preparing stock solution (1000 ppm) of Cr (VI) ions. Standard solution of the needed Cr (VI) concentration was prepared by suitable dilution. The initial and final chromium (VI) ions concentrations were spectrophotometrically determined using diphenyl carbazide. In other words, we aimed at dissolving 0.025 g of the powdered 1,5- diphenyl carbazide in 10 mL of acetone. Afterwards, it was to 10 mL of the solution that we aimed at adding 0.1 mL of the reagent and also one drop of the concentrated nitric acid. It is worth mentioning that the solution was comprised of less than 2 mg/L of chromium (VI) ions. The absorbance of the purple colored complex solution was read at 540 nm (ASTM, 2007). The developed color intensity can be connected to the hexavalent chromium concentration.

In order to find optimum parameters – i.e. adsorbent dose, etc. We aimed at performing batch adsorption studies. It was in 25 mL conical flask that the experiments were performed by mixing a specific amount of the adsorbent with 10 mL of Cr (VI) solution at the desired pH and contact time. The mixture was then shaken in the incubator at 25± 0.2 ^{o}C. Having centrifuged the solution, the supernatant was analyzed for final chromium concentration applying calibration curve of Cr (VI) standard solution. It is worth mentioning that the we repeated the experiments three times. The average and standard deviation of the results were calculated. Equation 1 represents the calculation of chromium ions removal percentage(%R) for each experiment:

$$\text{Removal}(\%) = \frac{(C_0 - C_e)}{C_0} \times 100 \quad (1)$$

C_0(mg.L^{-1}) and C_e stand for the initial and equilibrium Cr (VI) ions concentrations. Moreover, the Cr (VI) amount was evaluated, Equation 2:

$$q_e = \frac{(C_0 - C_e)}{m} \times V \quad (2)$$

Herein, q_e (mg.g^{-1}) is adsorption capacity, m (g) can be regarded as the mass of adsorbent, and V (L) is the volume of solution.

RESULTS AND DISCUSSION

In order to measure the distribution and particle size, the obtained aqueous solution of keratin was employed. In this sense, 63.7 nm was found to be the keratin particles average size (Fig. 1).

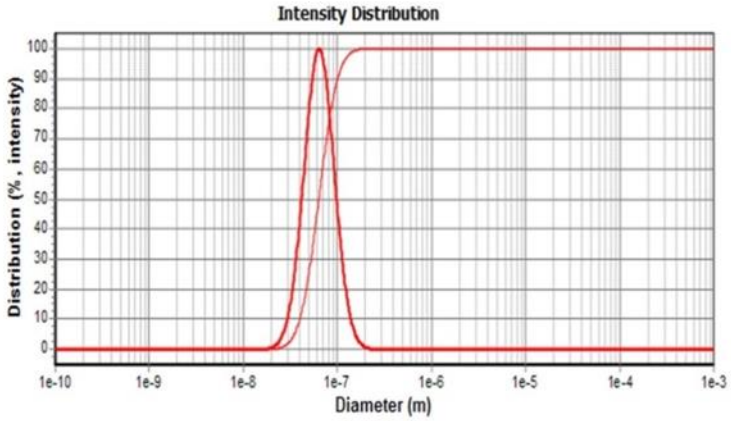

Figure 1. Particle size analysis for keratin nanoparticles.

Transmission electron microscopy (TEM) was applied to observe the structure of keratin nanoparticles providing direct morphology observation and the-keratin nanoparticle average size. Fig. 2 illustrates keratin nanoparticles TEM image in which the keratin nanoparticles average size was found to be below 100 nm. This result is greatly comparable to the result of particle size distribution.

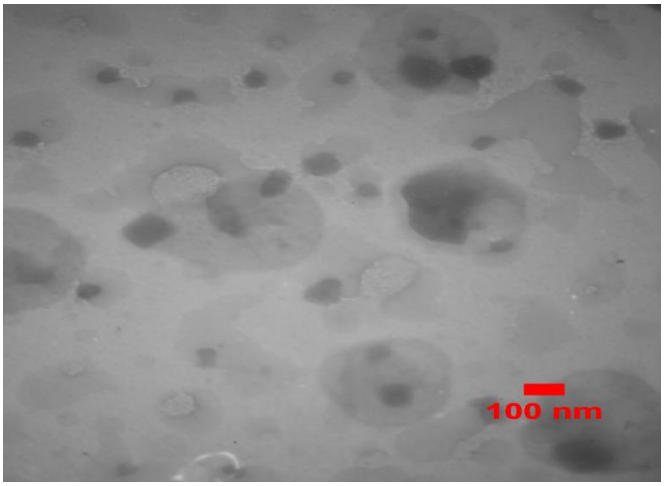

Figure 2. TEM micrograph of the keratin nanoparticles.

Comparisons between the human hair SEM photographs before and after keratin extraction showed that the human hair keratin was completely extracted and only the cuticle scale remained (Fig. 3). Moreover, keratin SEM photographs indicated a structure with a high porosity which was suitable for the adsorption of different species. It was seen that after the adsorption of Cr (VI), the pores and the surface of keratin nanoparticles had been changed (Fig. 4).

According to Fig. 5, the peak structure was demonstrated by FT-IR spectrum for keratin nanoparticles. The absorption regions –amides I, II, III and N-H stretching modes – were indicated by the modes related to peptide bonds(-CONH-). N-H stretching modes which can be regarded as a broad transition arise around 3297/cm. C=O stretching vibration mode can be found in Amide I which occurs at 1654/cm. Amide II occurring at 1540/cm, Amide II consists

of N-H bending vibration and C-C and C-N stretching. Amide III which would occur between 1220 and 1300/cm can be regarded as a complex absorption arising from the in-phase combinations of N-H in-plane bending, C=O bending vibration, C-N stretching, and C-C stretching vibration It is around 2880/cm that the related modes of methyl groups would occur. O-H stretching vibration would be demonstrated by the broad peak occurring at 3297/ cm (Martin, J. M. Cardamone, Irwin, & Brown, 2011).

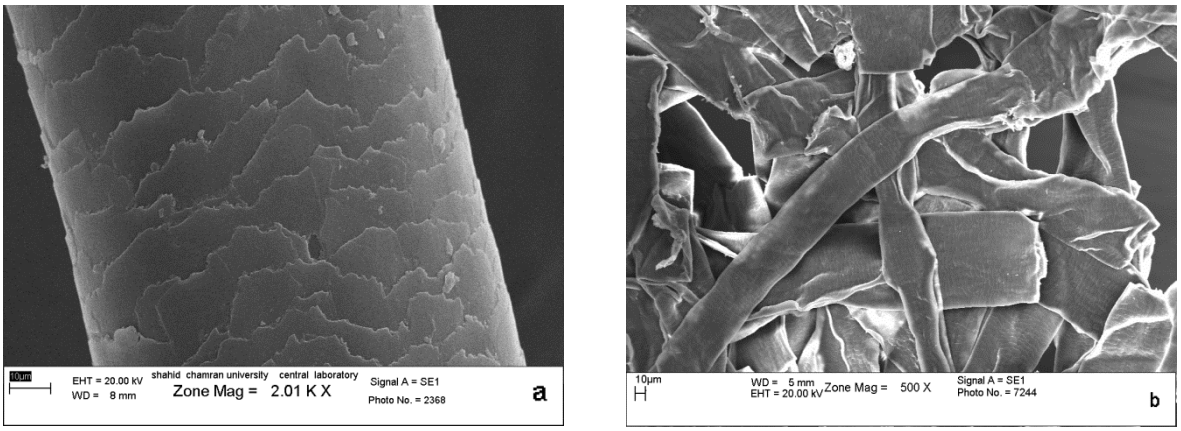

Figure 3. SEM micrograph of the human hair before (a) and after (b) keratin extraction

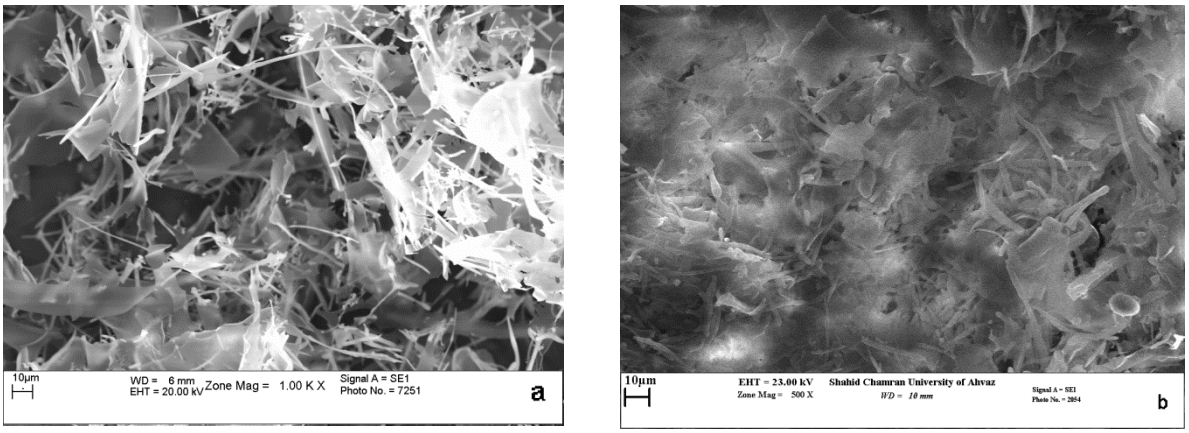

Figure 4. Keratin nanoparticles' SEM micrograph before (a) and after (b) Cr (VI) adsorption.

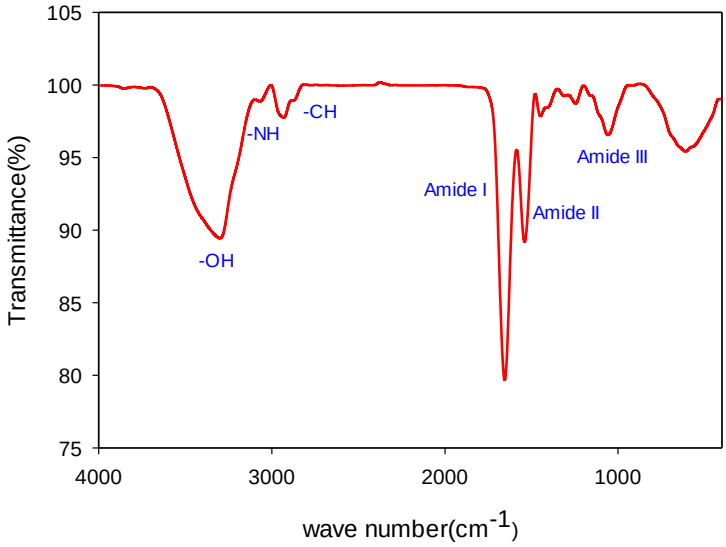

Figure 5. FT-IR spectra of keratin nanoparticles.

XRD pattern of the extracted keratin, in this work, presented a good agreement with the work reported by S. Li and X. Yang. The keratin nanoparticles exhibited a broad peak at and a small peak at, matching the-sheet structure (Li & Yang, 2014). Moreover, amorphous structure of keratin nanoparticles demonstrated a high surface area for increasing the adsorption capacity (Fig. 6).

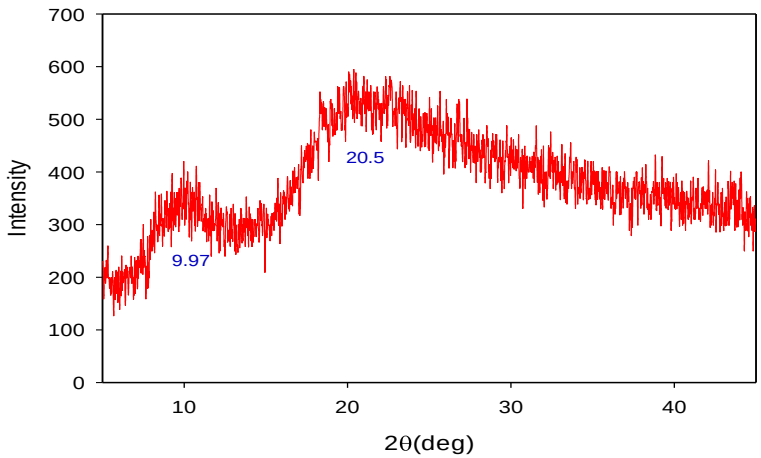

Figure 6. XRD pattern of keratin nanoparticles.

The pH of the initial solution can be regarded as the most significant parameter affecting the adsorption mechanism. Chromium exists in various oxidation states whose stability depends on the pH of the system. The dominant form of Cr (VI) at low pH value is. Increasing the pH value results in shifting the form to and (Javadian, Ahmadi, Ghiasvand, Kahrizi, & Katal, 2013). Fig. 7 shows that the adsorption capacity of the keratin nanoparticles was calculated for 24 hours in Cr (VI) aqueous solution with an initial concentration of 50 mg/L of Cr (VI) at different pH from 1 to 6. The highest adsorption capacity arises in pH 3, because in this pH keratin nanoparticles are under its isoelectric point, and an abundant

number of cationic sites exist in the amino acid side chains and the terminal groups. These sites are capable bind negative ions (A. Aluigi et al., 2012).

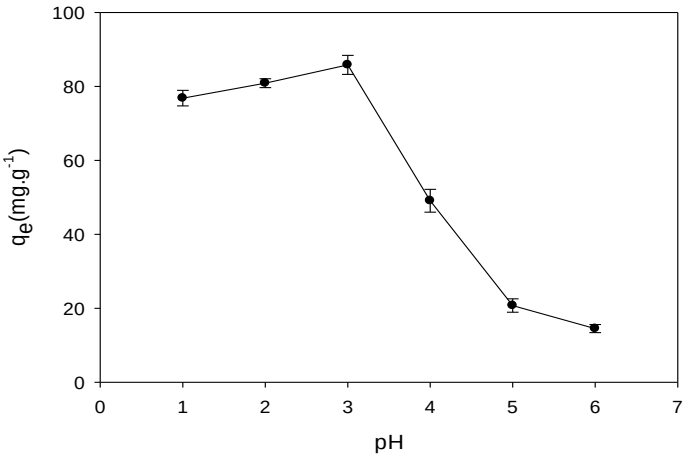

Figure 7. pH effect on Cr (VI) adsorption on keratin nanoparticles. (C_0=50 mg/L, adsorbent dose=0.3 g/L, contact time=24 h)

Various adsorbent doses from 0.002 to 0.014 g were applied to study the Cr (VI) ions removal via keratin nanoparticles in the aqueous solution. The removal efficiency and adsorption capacity are shown in Fig. 8. As seen, when the number of keratin nanoparticles solution increases, it results in decreasing the removal efficiency. It is so because of the fact that, on the keratin surface, hydrophobic functional groups are present, causing difficulties in absorbing Cr(VI) ions on keratin nanoparticles(Kar & Misra, 2004). Herein, the adsorbent amount was selected to be 0.003 g for the next experiments.

The Cr (VI) adsorption capacity at different times from 1to 48 hours was calculated in order to optimize the adsorption mechanism. Fig. 9 shows the Cr (VI) ions adsorption kinetic curve for the amount of 0.003 g keratin nanoparticles in various initial concentrations at pH 3. We witnessed a rapid adsorption but, then, the adsorption capacity slowly increased within the next 24 hours. Accordingly, due to the effect of contact time on Cr (VI), we considered 24h as the optimum time for the batch studies.

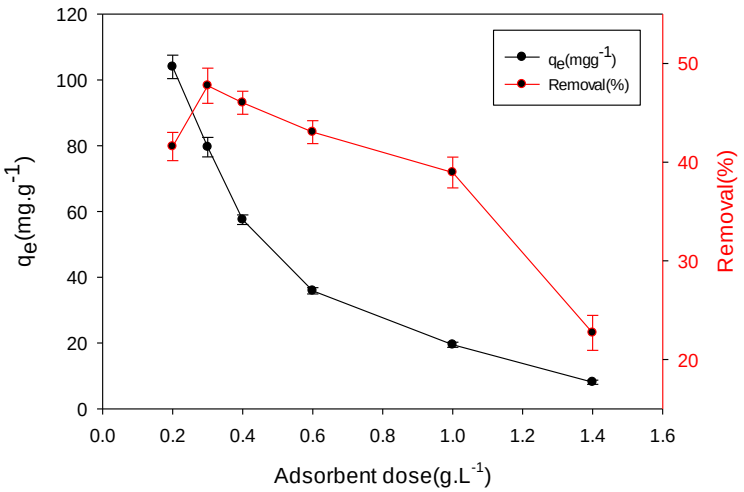

Figure 8. Effect of adsorbent dosages on Cr (VI) adsorption using keratin nanoparticles. (C_0=50 mg/L, pH=3, contact time=24 h)

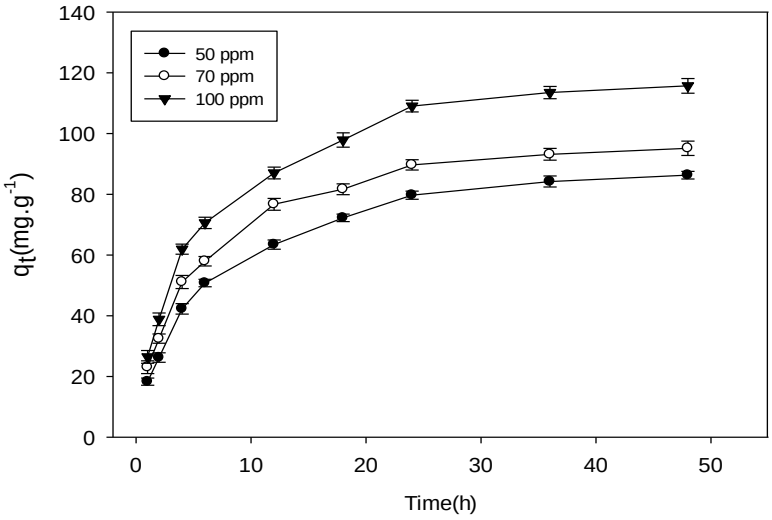

Figure 9. Effect of contact time on Cr (VI) adsorption using keratin nanoparticles. (pH=3, adsorbent dose=0.3 g/L) Cr (VI) Initial Concentration

Isotherm adsorption studies were performed by various Cr (VI) concentrations from 10 to 150 mg/L. Fig. 10 demonstrates that the adsorption capacity of the keratin nanoparticles increases along with increasing the initial concentration of Cr (VI). In this sense, it is at high initial concentration that it can be described by the presence of a large driving force for mass transfer.

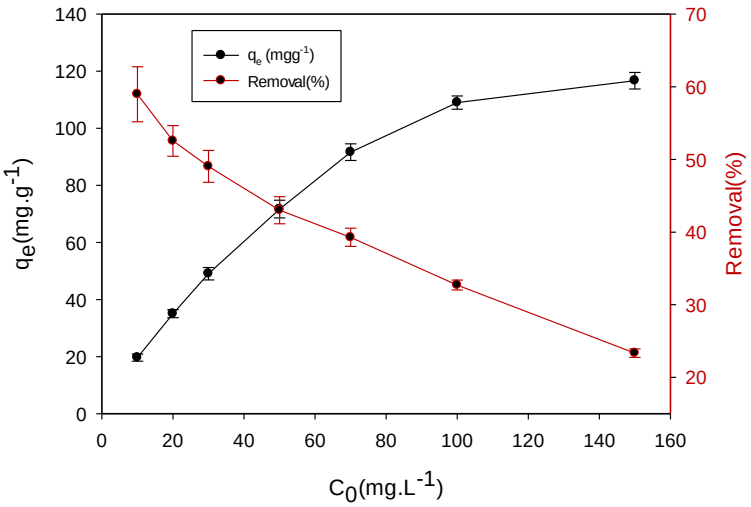

Figure 10. The initial concentration effect on the adsorption of Cr (VI) applying Keratin nanoparticles in optimum condition.

There are two possible reasons for Cr (VI) adsorption on keratin nanoparticles. First, the presence of the oxygen and nitrogen atoms in keratin structure was confirmed by FT-IR study and that their lone pair electrons could directly coordinate to the unoccupied 3d orbital of Cr(VI) (Vetriselvi & Santhi, 2015). Second, it is at low pH conditions that electrostatic interaction between the negatively charged chromium species such as $HCrO_4^-$ and CrO_4^{2-} with carboxyl and amide functional groups on keratin surface are mostly protonated. Conversely, functional groups deprotonation occurs at high pH and also the decrease of Cr(VI) adsorption can be resulted from the decrease of adsorption of Cr repulsion between the negative charge (Tahri Joutey, Sayel, Bahafid, & El-Ghachtouli, 2015).

In modeling the adsorption behavior, we aimed at testing the experimental data which were obtained from the initial Cr (VI) concentration effect on the adsorption capacity of the keratin nanoparticles applying the Langmuir, Freundlich and Temkin isotherms. Monolayer adsorption is emphasized by the Langmuir isotherm. Equation 3 shows the linear form of the Langmuir isotherm, as follows:

$$\frac{C_e}{q_e} = \frac{1}{q_m b} + \frac{C_e}{q_m} \tag{3}$$

where, is the concentration of the equilibrium ion in solution, is the maximum adsorption capacity, and is the Langmuir constant, corresponding to the adsorption energy (Langmuir, 1916). Fig. 11a shows the linear plots of the versus by which and values are calculated from the slope and intercept. Table 1 represents the obtained data. It is worth mentioning that it was in the Langmuir model that the maximum adsorption capacity was found to be 161.29 mg/g.

The experimental data on adsorption fitted the Freundlich adsorption isotherm. There exists a clear connection between the Freundlich model and the multilayer adsorption mechanism on the heterogeneous surface. Moreover, it is in the heterogeneous surface that the metal ion's adsorption energy would bind to an adsorbent site (Freundlich, 1906). Equation 4 shows the Freundlich model in a linearized form:

$$\ln q_e = \ln K_f + \frac{1}{n} \ln C_e \tag{4}$$

where, $n$andK_f can be related to adsorption intensity and adsorption capacity, The slope and intercept of the $ln\, q_e$as opposed to the$ln\, C_e$resulted in obtaining the n and K_f values (Fig. 11b, Table 1).

The factor in Temkin isotherm model is capable of considering the adsorbent and adsorbate interaction. Equation 5 presents the linear form:

$$q_e = B \ln A + B \ln C_e \tag{5}$$

The maximum binding energy $\left(\text{kJ.mol}^{-1}\right)$ is indicated by $B\, ln\, A$ (Temkin & Pyzhev, 1940).$A$and$B$are Temkin isotherm constants Fig. 11c shows the values of A ,B and b as illustrated in Table 1. Validity of each isotherm model is evaluated withR^2correlation coefficient and R^2_{adj} adjusted correlation coefficient for each model. Therefore, the experimental data have better agreement with the Freundlich isotherm model with$R^2 = 0.9934$.

The Cr (VI) ions adsorption capacity applying keratin nanoparticles was compared to the adsorbent reported in Table 2. In this sense, keratin nanoparticles have high performances comparable with the other sorbents such as the activated carbons from most of the materials. This might be attributed to the presence of the amino acids in keratin structure, acting as a suitable binding site for metal ions.

Table 1. Langmuir, Freundlich and Temkin isotherm parameters for Cr (VI) adsorption on keratin nanoparticles.

Isotherms	Parameters	Value
Langmuir	R^2	0.9910
	R^2_{adj}	0.9888
	$q_m(\text{mg.g}^{-1})$	161.29 ± 21.69
	$b(\text{L.mg}^{-1})$	0.030 ± 0.001
Freundlich	R^2	0.9934
	R^2_{adj}	0.9918

	K_f(mg.g^{-1})	8.51 ± 1.86
	n	1.60 ± 0.18
Temkin	R^2	0.9712
	R^2_{adj}	0.9640
	b(kJ.mol^{-1})	0.075 ± 0.018
	A(L.mg^{-1})	0.354 ± 0.276

$* \; x \pm t_{(n-2)} s_x (n = 6)$ P=0.05

Table 2. Comparison between Cr (VI) ions adsorption capacity applying keratin nanoparticles.

Adsorbent		References
Modified brown algae Sargassumbevanom	39.68	(Javadian et al., 2013)
Magnetic chitosan nanoparticle	55.80	(Thinh et al., 2013)
Nano porous activated neem bark	26.95	(Maheshwari & Gupta, 2015)
HK/PA 6 50/50 nanofiber mats	55.90	(A. Aluigi et al., 2012)
Tires activated carbon	58.50	(Hamadi, Dong Chen, M. Farid, & Q. Lu, 2001)
Soy hull biomass	7.28	(Blanes et al., 2016)
Keratin nanoparticles	161.29	This work

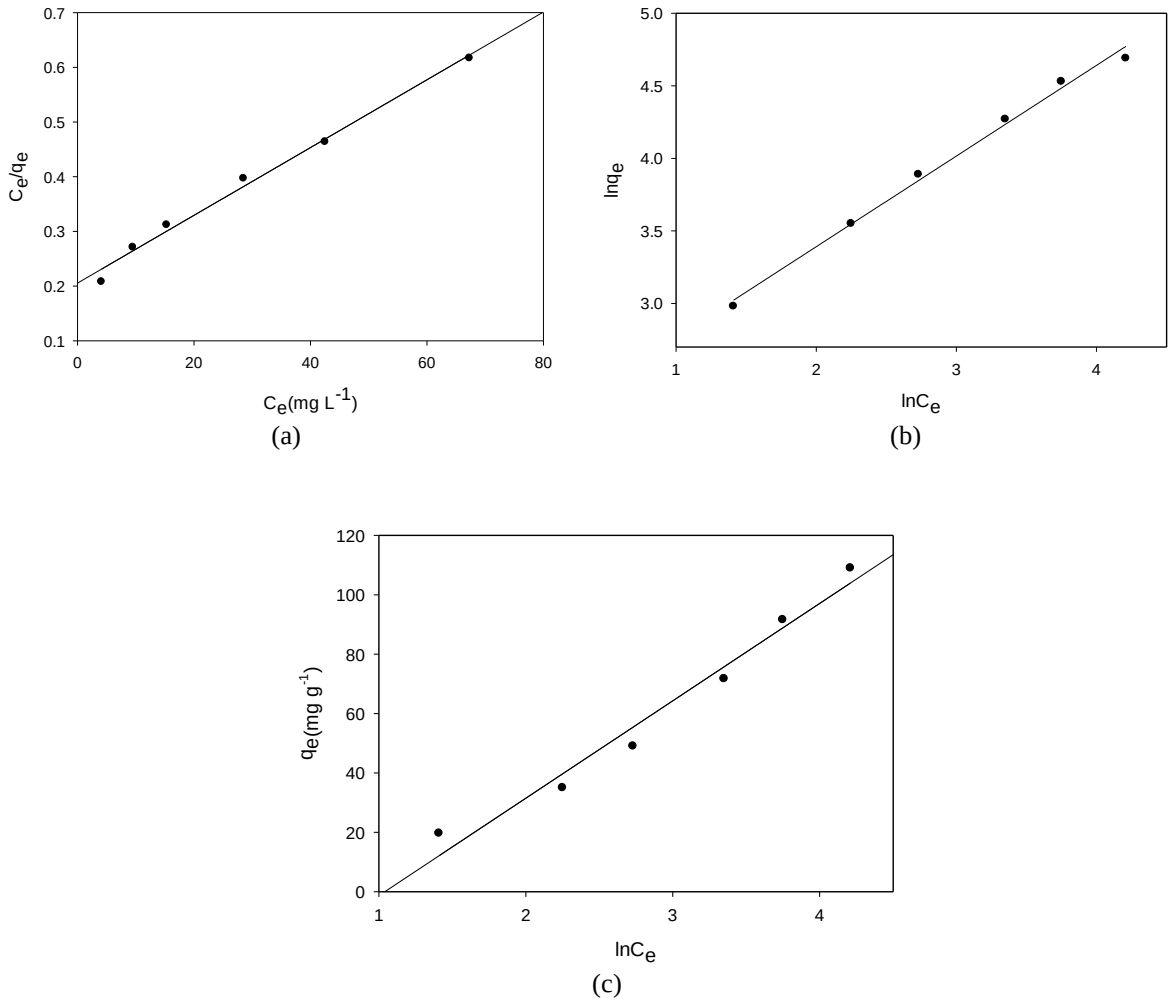

Figure 11. Linear plots of Isotherm models of (a) Langmuir, (b) Freundlich, and (c) Temkin for adsorption Cr (VI) on keratin nanoparticles at 298 K.

To study the mechanism of adsorption and potential rate-controlling steps, such as chemical reaction processes and mass transport, kinetic models have been employed to test the experimental data. In the current research, the Lagergren's first-order kinetic model, pseudo-second order kinetic model, Elovich model and the intraparticle diffusion model have been applied to the experimental data.

The Lagergren's first-order rate equation may have been the first one in describing the sorption of liquid-solid systems based on adsorbent capacity (Lagergrens, 1898). The linear form of Lagergren's first-order kinetic model is expressed by Equation 6:

$$\ln(q_e - q_t) = \ln q_e - k_1 t \tag{6}$$

where$q_e$andq_t $\left(\text{mg.g}^{-1}\right)$are adsorption capacity at equilibrium and at the time t, respectively. k_1 is the rate constant of pseudo-first-order kinetic model (See Fig. 12a).

The adsorption kinetics can also be described by a pseudo-second order kinetic model, and the linearized form of this model is given in Equation 7(Ho & Mc Kay, 1998):

$$\frac{t}{q_t} = \frac{1}{k_2 q_e^2} + \frac{t}{q_e} \tag{7}$$

wherek_2 $\left(\text{mg.g}^{-1}.\text{min}^{-1}\right)$ is the rate constant of Pseudo-second order kinetic model. The linear plot of t/q_tvs. t is shown in Fig. 12b. The$k_2$and$q_e$values are calculated from the slope and intercept of this plot, respectively. Kinetic parameters are calculated and shown in Table 3.
The nonlinear form of Elovich equation is defined by Equation 8:

$$\frac{dq_t}{dt} = \alpha \exp(-\beta q_t) \tag{8}$$

where,α $\left(\text{mg.g}^{-1}.\text{min}^{-1}\right)$ is the initial adsorption rate, andβ $\left(\text{g.mg}^{-1}\right)$is related to surface coverage area and activation energy of the chemisorption (Low, 1960). Rewriting Eq.8 at boundary condition provides the linear form of Elovich equation:

$$q_t = \frac{1}{\beta \ln(\alpha\beta)} + \frac{1}{\beta \ln t} \tag{9}$$

In whichα and $\beta$are determined from slope and intercept of the $q_t$verses$ln\ t$in Fig. 12c.The values ofα and β are presented in Table 3.

R^2, $R^2_{\text{adj}}$and Chi-square test was also done for the choice of best kinetic model with Equation 10(Srivastava, Sharma, & Sillanpaa, 2015):

$$\chi^2 = \sum^{\Sigma} \frac{(qcalc^2{}_{exp}}{q_{calc}} \tag{10}$$

The comparison between R^2 and R^2_{adj} values for these models demonstrates that the adsorption process was better fitted in the Pseudo-second order kinetic model with a higher correlation and lower degree of difference(χ^2). Table 3 indicates that χ^2 value is less for Pseudo-second order kinetic model, which helps the applicability of pseudo-second order kinetic model.

The Intraparticle diffusion model was expanded by Webber and Morris to study the mechanism of adsorption process in porous media. This model can be demonstrated by Equation 11(Weber, Morris, & Sanit, 1963):

$$q_t = k_{id} t^{0.5} + C_i \quad (11)$$

where, k_{id} is the Intraparticle diffusion rate constant of the ith step, and C_i is proportional to the thickness of the boundary layer. The plot of q_t versus $t^{0.5}$ is shown in Fig. 12d which illustrates three steps with various slopes, representing multi-step, restricted adsorption mechanism. The intraparticle diffusion constant for each step is given in Table 4. The results prove that the Cr (VI) ions diffuse rapidly between the keratin nanoparticles at the beginning of the adsorption mechanism and Cr (VI) ions diffuse into macropores. Subsequently, intraparticle diffusion slows down and Cr (VI) ions diffuse into micropores. Finally, the equilibrium state arrives.

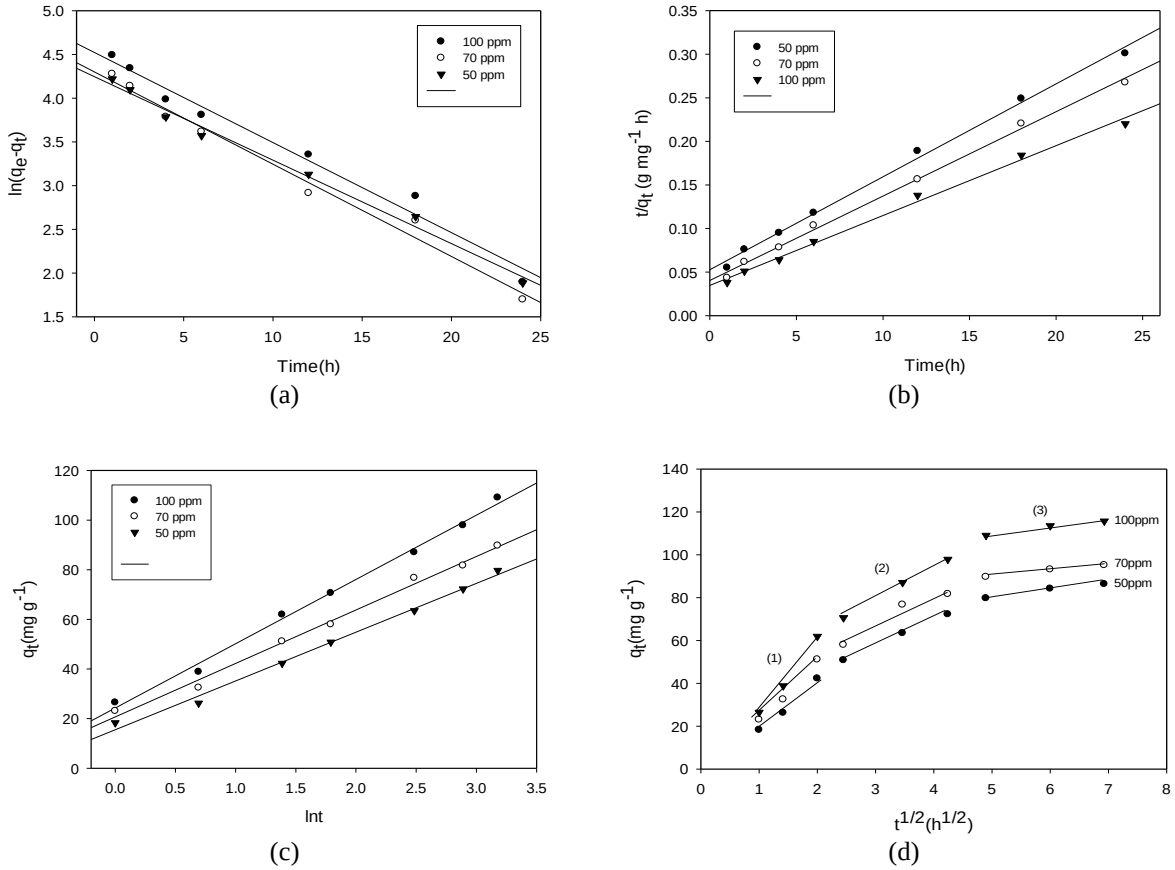

Figure 12. Kinetic models of (a) Pseudo-first order, (b) Pseudo-second order(c) the Elovich and (d) Intra-particle diffusion for adsorption Cr (VI) on keratin nanoparticles.

Table 3. Kinetic parameters for Cr (VI) adsorption by Keratin nanoparticles.

Model	C_0(mg.L^{-1})		
	50	**70**	**100**
Pseudo first-order			
$k_1(h^{-1})$	0.096 ± 0.011	0.106 ± 0.015	0.103 ± 0.017
$q_{e.calc}$(mg.g^{-1})	69.93 ± 9.65	73.75 ± 14.01	92.19 ± 20.02
$q$mg.g$^{-1}{}_{e.exp}$	86.32	95.18	115.73
R^2	0.9900	0.9846	0.9791
R^2_{adj}	0.9881	0.9816	0.9749
χ^2	3.84	6.23	6.01
Pseudo first-order			
$k_2(g.\text{mg}^{-1}.\text{h}^{-1})$	$2.1 \times 10^{-3} \pm 3 \times 10^{-4}$	$2.3 \times 10^{-3} \pm 4 \times 10^{-4}$	$1.9 \times 10^{-3} \pm 4 \times 10^{-4}$

$q_{e.calc}$(mg.g^{-1})	93.46 ± 7.41	103.09 ± 5.46	125.00 ± 12.04
$q$mg.g$^{-1}{}_{e.exp}$	86.32	95.18	115.73
R^2	0.9958	0.9969	0.9900
R^2_{adj}	0.9949	0.9963	0.9881
χ^2	0.55	0.61	0.69
Elovich			
α(mg.g^{-1}.h^{-1})	43.27 ± 6.51	56.27 ± 8.29	66.11 ± 8.70
$\beta(g$.mg$^{-1})$	0.051 ± 0.005	0.046 ± 0.004	0.039 ± 0.003
R^2	0.9937	0.9932	0.9947
R^2_{adj}	0.9924	0.9919	0.9936

Table 4. Intraparticle diffusion model parameter for Cr (VI) adsorption by Keratin nanoparticles.

Step	50 ppm			70 ppm			100 ppm		
	R^2	k_{id}	C_i	R^2	k_{id}	C_i	R^2	k_{id}	C_i
1	0.9913	24.22	-6.71	0.9920	28.30	-6.11	0.9946	35.77	-10.22
2	0.9992	11.99	21.57	0.9395	13.49	26.46	0.9983	15.26	33.51
3	0.9746	3.28	63.95	0.9882	2.71	76.60	0.9792	3.31	93.12

The effect of temperature on the adsorption of Cr (VI) ions on keratin nanoparticles was investigated by conducting experiments for the initial Cr (VI) ions concentrations at 293, 303, 313 and 323 K. It was observed that by increasing the temperature, the removal percentage of Cr (VI) ions increased. The mechanism of Cr (VI) adsorption is illustrated by the following reversible process, which happens in the heterogeneous surface at the equilibrium state:

Cr (VI) in solution ↔Cr (VI) on adsorbent (12)

The thermodynamic equilibrium constant (K_C) for adsorption process was determined, using Equation 13:

$$K_C = \frac{C_a}{C_e} \tag{13}$$

Here, C_a and C_e are the Cr (VI) concentration on the adsorbent and the solution at equilibrium, respectively. The thermodynamic equilibrium constant is related to Gibbs free energy change using the Van't Hoff equation.

$$\Delta G^0 = -RT \ln K_C \tag{14}$$

where, ΔG^0 (J.mol^{-1}) is standard Gibbs free energy change R (J.mol$^{-1}K^{-1}$) is universal gas constant and $T(K)$ is the temperature of the adsorption process. According to the thermodynamic relationship, Gibbs free energy change is dependent on the enthalpy and entropy changes of adsorption at a constant temperature.

$$\Delta G^0 = \Delta H^0 - T\Delta S^0 \tag{15}$$

Equation 17 is obtained from the merger of Equations 14 and 15.

$$\ln K_C = \frac{\Delta S^0}{R} - \frac{\Delta H^0}{RT} \tag{16}$$

The values of ΔH^0 and ΔS^0 were determined from the slope and intercept of the plot of $ln\ K_C$ versus $1/T$. As can be seen in Fig. 13 and presented data in Table 5, ΔG^0 was obtained to be negative, which indicates the spontaneity and feasibility of adsorption process. The positive value of ΔH^0 confirmed the endothermic nature of adsorption process.

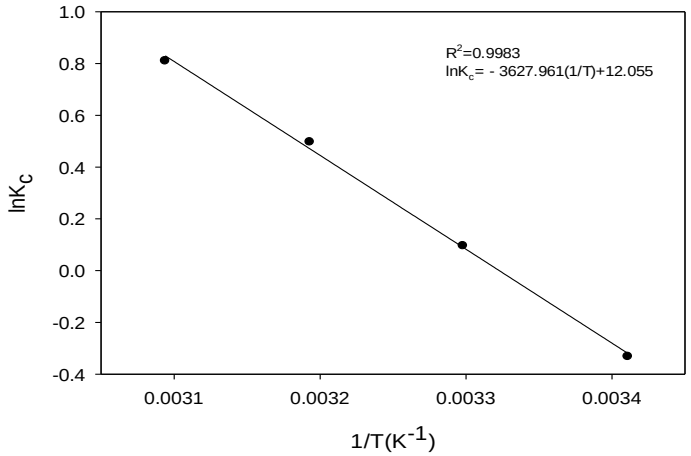

Figure 13. The Van'thoff plot for adsorption Cr (VI) on keratin nanoparticles.

Table 5. Thermodynamic parameters for the adsorption of Cr (VI) on keratin nanoparticles.

$-\Delta G^0$ (kJ.mol^{-1})				ΔH^0 (kJ.mol^{-1})	ΔS^0 (J.mol$^{-1}K^{-1}$)
$20°C$	$30°C$	$40°C$	$50°C$		
-0.81	0.24	1.29	2.18	30.16 ± 3.81	100.22 ± 12.37

$* \; x \pm t_{(n-2)} s_x (n = 4)$ P=0.05

CONCLUSION

A novel application of biocompatible and biodegradable keratin nanoparticles, which were prepared from human hair waste as bioresources, for the removal of Cr (VI) from the aqueous solutions was investigated. The characterization tests revealed that the extracted keratin nanoparticles had porous structure with a high surface area, making it suitable for the removal of heavy metal ions such as Cr (VI). Batch adsorption studies were performed in order to find the optimum parameters. The adsorption capacity was extremely pH-dependent, and the maximum adsorption of Cr (VI) happened in the acidic pH range. Pseudo-second order kinetic model governed the adsorption process and the intraparticle diffusion model was found as the major mechanism controlling the rate of the Cr (VI) adsorption on the keratin nanoparticles. The adsorption manner was better described with the Freundlich isotherm models. The maximum adsorption capacity for keratin nanoparticles was obtained to be 161.29 mg/g that is comparable or better than other adsorbents. Thermodynamic studies indicated that the Cr (VI) adsorption by keratin nanoparticles had a spontaneous and endothermic nature.

GRANT SUPPORT DETAILS

The present research did not receive any financial support.

CONFLICT OF INTEREST

The authors declare that there is not any conflict of interests regarding the publication of this manuscript. In addition, the ethical issues, including plagiarism, informed consent,

misconduct, data fabrication and/ or falsification, double publication and/or submission, and redundancy has been completely observed by the authors.

LIFE SCIENCE REPORTING

No life science threat was practiced in this research.

REFERENCE

Aluigi, A., Tonetti, C., Vineis, C., Tonin, C. and Mazzuchetti, G. (2011). Adsorption of copper (II) ions by Keratin/PA6 blend nanofibres. *Euro. Pol J., 47*(9), 1756-1764.

Aluigi, A., Tonetti, C., Vineis, C., Varesano, A., Tonin, C. and Casasola, R. (2012). Study on the Adsorption of Chromium (VI) by Hydrolyzed Keratin/Polyamide 6 Blend Nanofibres. *Journal of Nanoscience and Nanotechnology, 12 ,No 9*, 7250-7259.

ASTM. (2007). Standard Test Methods for Chromium in Water. *Annual Book of ASTM Standards, D1687-02*.

Bansal, M., Singh, D. and Garg, V. K. (2009). A comparative study for the removal of hexavalent chromium from aqueous solution by agriculture wastes' carbons. *Journal of Hazardous Materials, 171*, 83–92.

Blanes, P. S., Bordoni, M. E., Gonzalez, J. C., Garcia, S. I., Atria, A. M., Sala, L. F. and Bellu, S. E. (2016). Application of soy hull biomass in removal of Cr(VI) from contaminated waters, Kinetic, thermodynamic and continuous sorption studies. *Journal of Environmental Chemical Engineering, 4*, 516-526.

Cui, M., Song, G., Wang, C. and Song, Q. (2015). Synthesis of cysteine-functionalized water-soluble luminescent copper nanoclusters and their application to the determination of chromium(VI). *Microchim Acta, 182*, 1371–1377.

Dehghani, M. H., Sanaei, D., Ali, I. and Bhatnagar, A. (2016). Removal of chromium (VI) from aqueous solution using treated waste newspaper as a low-cost adsorbent: Kinetic modeling and isotherm studies. *Journal of Molecular Liquids, 215*, 671-679.

Freundlich, H. M. F. (1906). Over the Adsorption in Solution. *Journal of Physical Chemistry, 57*, 385–470.

Ghosh, A. and Collie, S. R. (2014). Keratinous Materials as Novel Absorbent Systems for Toxic Pollutants. *Defence Science Journal, 64*(3), 209-221.

Gupta, A. (2014). Human Hair"Waste" and Its Utilization:Gaps and Possibilities. *Journal of Waste Management, 2014*, 1-17.

Hamadi, N. K., Dong Chen, X., M. Farid, M. and Q. Lu, M. G. (2001). Adsorption kinetics for the removal of chromium (VI) from Aqueous solution by adsorbents derived from used tyres and sawdust. *Chemical Engineering Journal, 84*, 95-105.

Hearle, J. W. S. (2000). A critical review of the structural mechanics of wool and hair fibres. *International Journal of Biological Macromolecules, 27(2)*, 123-138.

Ho, Y. S. and Mc Kay, G. (1998). A comparison of chemisorption kinetic models applied to pollutant removal on various sorbents. *Institution of Chemical Engineers 76, Part B*, 332-340.

Javadian, H., Ahmadi, M., Ghiasvand, M., Kahrizi, S. and Katal, R. (2013). Removal of Cr(VI) by modified brown algae Sargassum bevanom from aqueous solution and industrial wastewater. *Journal of the Taiwan Institute of Chemical Engineers, 44*, 977-989.

Kar, P. and Misra, M. (2004). use of keratin fiber for separation of heavy metals from water. *J. Chemical Technol. Biotechnol., 79*(11), 1313-1319.

Khosravi, R., Fazlzadehdavil, M., Barikbin, B. and Taghizadeh, A. A. (2014). Removal of hexavalent chromium from aqueous solution by granular and powdered Peganum Harmala. *Applied Surface Science, 292*, 670-677.

Lagergrens. (1898). About the Theory of So-Called Adsorption of Soluble Substances. *KUNGLIGA SVENSKA VETENSKA PSAKADEMIENS HANDLINGAR, 24, No. 4*, 1-39.

Langmuir, L. (1916). The constitution and fundamental properties of solids and liquids *The Journal of the American Chemical Society 38*, 2221-2295.

Li, S. and Yang, X.-H. (2014). Fabrication and Characterization of Electrospun Wool Keratin/Poly(vinyl alcohol) Blend Nanofibers. *Advances in Materials Science and Engineering, 2014*, 1-7.

Liu, L., Leng, Y. and Lin, H. (2016). Photometric and visual detection of Cr(VI) using gold nanoparticles modified with 1,5-diphenylcarbazide. *Microchim Acta, 183*, 1367–1373.

Low, M. J. D. (1960). Kinetics of chemisorption of gases on solids. *Chemical Reviews, 60(3)*, 267-312.

Maheshwari, U. and Gupta, S. (2015). Removal of Cr(VI) from Wastewater Using a Natural Nanoporous Adsorbent: Experimental, Kinetic and Optimization Studies. *Adsorption Science & Technology, 33*, 171-188.

Marjan, T., Mohammad, T.Y., Zahra, B., Leily, H.S., Mohammad, N., Hojatollah, M., Mohsen, M., and Mojtaba, K. (2020) Carboxymethyl cellulose improved adsorption capacity of polypyrrole/CMC composite nanoparticles for removal of reactive dyes: Experimental optimization and DFT calculation. Chemosphere. 255, 127052.

Martin, J., J. M. Cardamone, J. M., Irwin, P. L. and Brown, M. (2011). Keratin capped silver nanoparticles-Synthesis and characterization of a nanomaterial with desirable handling properties. *Colloids and Surfaces B: Biointerfaces, 88*, 354-361.

Mohsen, M., Towan, K., Marjan, T., Mohammad, T.Y., Parnian, T., and Aseman, L. (2019). Facile green synthesis of silver nanoparticles using Crocus Haussknechtii Bois bulb extract: Catalytic activity and antibacterial properties. Colloid and Interface Science Communications, 33, 100211.

Nik Abdul Ghani, N.R., Jami, M.S.,and Alam, M.Z. (2021). The role of nanoadsorbents and nanocomposite adsorbents in the removal of heavy metals from wastewater: A review and prospect. Pollution, 7 (1), 153-179.

Qi, W., Zhao, Y., Zheng, X., Ji, M. and Zhang, Z. (2016). Adsorption behavior and mechanism of Cr(VI) using Sakura waste from aqueous solution. *Applied Surface Science, 360*, 470-476.

Rezvani, M., Asgharinezhad, A. A., Ebrahimzadeh, H. and Shekari, N. (2014). A polyaniline-magnetite nanocomposite as an anion exchange sorbent for solid-phase extraction of chromium(VI) ions. *Microchim Acta, 181*, 1887–1895.

Saboori, A. (2017). A nanoparticle sorbent composed of MIL-101(Fe) and dithiocarbamate-modified magnetite nanoparticles for speciation of Cr(III) and Cr(VI) prior to their determination by electrothermal AAS. *Microchim Acta, 184*, 1509–1516.

Sekimoto, Y., Okiharu, T., Nakajima, H., Fujii, T., Shirai, K. and Moriwaki, H. (2013). Removal of Pb(II) from water using keratin colloidal solution obtained from wool. *Environmental Science and Pollution Research*, 1727-1725.

Srivastava, V., Sharma, Y. C. and Sillanpaa, M. (2015). Responce surface methodological approach for the optimization of adsorption process in the removal of Cr(VI) ions by $Cu_2(OH)_2CO_3$ nanoparticles. *Applied Surface Science, 326*, 257-270.

Tahri Joutey, N., Sayel, H., Bahafid, W. and El-Ghachtouli, N. (2015). Mechanisms of Hexavalent Chromium Resistance and Removal by Microorganisms. *Reviews of Environmental Contamination and Toxicology, 233*, 45-66.

Temkin, M. I. and Pyzhev, V. (1940). Kinetics of mmonia synthesis on promoted iron catalysts. *Acta Physiochim USSR, 12*, 327-356.

Thinh, N., Bich Hanh, P. T., Thanh Ha, L. T., Ngoc Anh, L., Vinh Hoang, T., Hoang, V. D. and Dai Lam, T. (2013). Magnetic chitosan nanoparticles for removal of Cr(VI) from aqueous solution. *Materials Science and Engineering C, 33*, 1214-1218.

Vetriselvi, V. and Santhi, R. J. (2015). Redox polymer as an adsorbent for the removal of chromium (VI) and lead (II) from the tannery effluents. *Water Resources and Industry, 10*, 39-52.

Volkov, V. and Cavaco-Paulo, A. (2016). Enzymatic phosphorylation of hair keratin enhances fast adsorption of cationic moieties. *International Journal of Biological Macromolecules, 85*, 476-486.

Weber, W. J., Morris, J. C. and Sanit, J. (1963). Kinetics of Adsorption on Carbon from Solution. *Journal of the Sanitary Engineering Division, 89*, 31-59.

Xie, J., Gu, X., Tong, F., Zhao, Y. and Tan, Y. (2015). Surface complexation modeling of Cr(VI) adsorption at the goethite–water interface. *Journal of Colloid and Interface Science, 455*, 55–62.

Zhang, H., Huang, Y., Hu, Z., Tong, C., Zhang, Z. and Hu, S. (2017). Carbon dots codoped with nitrogen and sulfur are viable fluorescent probes for chromium(VI). *Microchim Acta, 184*, 1547–1553.